Functional expression of the ATP-gated P2X7 receptor in human iPSC-derived astrocytes

Jaideep Kesavan
RCSI University of Medicine and Health Sciences
Orla Watters
SETU Waterford
Laura Diego-Garcia
Complutense University of Madrid
Aida Menendez Mendez
RCSI University of Medicine and Health Sciences
Mariana Alves
RCSI University of Medicine and Health Sciences
Klaus Dinkel
Lead Discovery Center GmbH
Michael Hamacher
Affectis Pharmaceuticals AG
Jochen H. M. Prehn
RCSI University of Medicine and Health Sciences
David C. Henshall
RCSI University of Medicine and Health Sciences
Tobias Engel (tengel@rcsi.ie)
RCSI University of Medicine and Health Sciences

Short Report

Keywords: P2X7 receptor, hiPSC-derived astrocytes, ATP and BzATP-evoked Ca2+ fluctuations

Posted Date: March 20th, 2023

DOI: https://doi.org/10.21203/rs.3.rs-2693543/v1

Abstract

The P2X7 receptor (P2X7R) is a cation-permeable ionotropic receptor activated by extracellular adenosine 5'-triphosphate (ATP) which has been implicated in numerous diseases of the CNS, including epilepsy. Activation of the P2X7R can trigger diverse responses including the release of pro-inflammatory cytokines, modulation of neurotransmission, cell proliferation or cell death. There have been conflicting reports on the cellular identity of P2X7R-expressing cells in the brain. Expression of P2X7Rs is well documented on microglia and oligodendrocytes but the presence of P2X7Rs on astrocytes remains debated. Furthermore, most functional studies on P2X7R responses have used cells from rodents or immortalised cell lines expressing human P2X7Rs. To assess the endogenous and functional expression of P2X7Rs in human astrocytes, we differentiated human-induced pluripotent stem cells (hiPSCs) into GFAP and S100 β-expressing astrocytes. Immunostaining revealed prominent punctate P2X7R staining on hiPSC-derived astrocytes and P2X7R protein expression was also confirmed by Western blot analysis. Importantly, stimulation with the potent nonselective P2X7R agonist BzATP or endogenous agonist ATP induced robust calcium rises in hiPSC-derived astrocytes which were blocked by the selective P2X7R antagonists AFC-5128 or JNJ-47965567. Our findings provide evidence for the functional expression of P2X7Rs in hiPSC-derived astrocytes and support their *in vitro* utility in investigating the role of the P2X7R and drug screening in disorders of the CNS.

Introduction

The adenosine triphosphate (ATP)-gated purinergic P2X7 receptor (P2X7R) plays a pivotal role in ATP-mediated signal transmission in the brain. The P2X7R belongs to the cationic P2X receptor family, forming a membrane channel and responding to extracellularly-released ATP [1, 2]. ATP may be released from nerve terminals or glial cells by exocytosis or from astroglial cells via non-exocytotic mechanisms. ATP has also been shown to leak through the damaged neuronal or glial plasma membrane during brain injury [3, 4]. When ATP binds to the extracellular domain of the P2X7R, the channel opens, allowing the permeation of small cations such as Na^+, Ca^{2+}, and K^+ [5]. In addition, P2X7Rs are also believed to form a non-selective "macro pore" which allows the influx of large-molecular-weight molecules [5]. The downstream consequences of P2X7R signaling are dependent on the cellular location of the expressed receptor and various non-cell autonomous effects have been reported. Activation of the P2X7R on microglia leads to the release of pro-inflammatory mediators such as interleukin-1β (IL-1β), IL-6, and tumor necrosis factor-α (TNF-α), triggering neuroinflammation [6]. In contrast, the presence and effects of P2X7Rs on other brain cell types is less certain. Activation of the P2X7R on astrocytes has been reported to evoke glutamate release leading to potential excitotoxic effects [7–10]. Astrocyte-mediated P2X7R responses may, however, also be important for the release of pro-inflammatory cytokines such as IL-1β, IL-6, and TNF-α, thereby contributing to pathologies [11]. However, other studies have failed to detect the P2X7R on this cell type [12–14].

Due to its distinct characteristics, including its relatively low affinity for ATP and its prominent role in driving inflammatory processes, the P2X7R has attracted considerable interest as a potential target for

various central nervous system (CNS) disorders such as epilepsy, neurodegenerative diseases, migraine and neuropathic pain [15, 16]. P2X7R protein expression has been found to be up-regulated in the brain of patients with different neurological diseases and P2X7R antagonism has shown benefits in multiple animal models of brain diseases (e.g. epilepsy, schizophrenia, depression) [17–21].

Despite the 80% sequence homology between human and murine P2X7Rs, differences in the receptor sensitivity towards various ligands have been described. For example, the human P2X7R has been shown to be 10–100 times more sensitive to the non-selective agonist 2', 3'-O-(benzoyl-4-benzoyl)-adenosine 5'-triphosphate (BzATP) compared to the murine ortholog [22]. KN-62 (1-[N,O-bis(5-isoquinolinesulphonyl)-N-methyl-L-tyrosyl]-4-phenylpiperazine), a potent antagonist for human P2X7Rs, has been shown to be inefficacious at rat P2X7Rs [23]. Likewise, human P2X7Rs exposed to ivermectin, a broad spectrum anti-parasitic agent, underwent positive allosteric modulation while modest results were seen at rodent P2X7Rs, suggesting a species-specific mode of action [24]. GW791343 is a negative modulator at the human P2X7R, but a positive modulator at rat P2X7Rs [25]. Thus, P2X7Rs exhibit remarkable species-specific differences in the pharmacological properties including agonist and antagonist potency and sensitisation which could account for the failure in clinical translation of the results from animal models [26]. Consequently, there is an increasing need for the investigation of the expression and function of P2X7Rs in human brain-relevant models.

Resected human primary brain tissue is very scarce and often shows alterations associated with pathology. Advances in induced pluripotent stem cell (iPSC) technology has led to the differentiation of region-specific human neurons, astrocytes, oligodendrocytes and microglia from somatic cells [27–30]. These iPSC-derived human neurons and glia have demonstrated their potential for the investigation of human neuronal development *in vitro*, pharmacological screening and assessing phenotypic alterations in patient-specific iPSC-derived neural cells [31–36].

In rodent brain, although P2X7Rs are preferentially localized on microglia, they are also expressed on other cell types (e.g. oligodendrocytes and most possibly on astrocytes and neurons) despite at a lower density. Importantly, P2X7R-mediated effects via astrocytes have been suggested to contribute to disease progression in several brain diseases [37, 38]. To date, only a few studies have, however, addressed the functional expression of the P2X7R in human primary astrocytes compared with work on rodent counterparts [39–41]. Here, we demonstrate the expression of P2X7Rs in hiPSC-derived astrocytes, thereby establishing a model for the investigation of functional P2X7Rs in a human system.

Methods

Culture and differentiation of hiPSCs

hiPSC line HPSI0114i-eipl_1 (ECACC 77650081; Culture Collections, Public Health England, UK), made by reprogramming with non-integrating virus from skin fibroblasts from a healthy individual at passage 32, were maintained under feeder-free conditions on vitronectin (STEMCELL Technologies, British Columbia,

Canada)-coated 6-well plates in E8 medium (Thermo Fisher Scientific, Massachusetts, U.S.A). The hiPSCs were dissociated by using 0.5 mM EDTA for 2 min at 37°C, and reseeded at the density of 1×10^4 cells per cm^2. For the neural induction of hiPSCs, approximately 24 h after splitting, culture medium was switched to Gibco PSC Neural Induction Medium (Thermo Fisher Scientific, Massachusetts, U.S.A) containing Neurobasal medium and Gibco PSC neural induction supplement. Neural induction medium was changed every other day from day 0 to day 4 of neural induction and every day thereafter. At day 10 of neural induction, primitive NSCs (pNSCs) were dissociated with Accutase (Thermo Fisher Scientific, Massachusetts, U.S.A) and plated on Geltrex-coated dishes at a density of 1×10^5 cells per cm^2 in NSC expansion medium containing 50% Neurobasal medium, 50% Advanced DMEM/F12, and 1% neural induction supplement (Thermo Fisher Scientific, Massachusetts, U.S.A). pNSCs were passaged on the 4th day at a 1:3 split ratio to derive NSCs and cells at passage 4 were used for the differentiation of glia. For astrocyte differentiation, pNSCs were plated onto Geltrex-coated coverslips at a density of 5×10^4 cells per cm^2 in an astrocyte differentiation medium (DMEM supplemented with 1% fetal bovine serum, 1% sodium pyruvate, 1% non-essential amino acids, 0.5% G-5 supplement (all from Thermo Fisher Scientific, Massachusetts, U.S.A)) for 5 days. The astrocytes were passaged at a split ratio of 1:2 and medium was changed every 3 days. Astrocytes were used for experimentation at passage 7 to 10.

Immunocytochemistry

Astrocytes cultured on coverslips were fixed with 4% paraformaldehyde (PFA) or a combination of acetic acid (6.71%) and ethanol (62.5%) for 15 min. After 3 washes in phosphate buffered saline, cells were permeabilised with 0.1% Triton for 20 min and blocked in 1% BSA for 30 min. Cells were incubated at 4°C overnight in primary antibody diluted in 1% BSA. The cells were then incubated in secondary antibody diluted in 1% BSA for 1 h at room temperature. The following primary antibodies were used: mouse anti-GFAP (Merck, Missouri, United States, dilution 1:200), mouse anti-S100β (Abcam, Cambridge, UK, dilution 1:200) and rabbit anti-P2X7R (Alomone Labs, Jerusalem, Israel, dilution 1:200). The respective secondary antibodies were conjugated to Alexa Fluor 488 or Alexa Fluor 594 (Thermo Fisher Scientific, Massachusetts, U.S.A) and used at a dilution of 1:1000. The nuclei were counterstained with 10 μM Hoechst (Merck, Missouri, United States). Coverslips were mounted and images were acquired using a Leica DM4000B fluorescence microscope.

Drug application

Stock solutions of BzATP (Alomone Labs, Jerusalem, Israel), ATP (Merck, Missouri, United States), AFC-5128 [42] and JNJ-47965567 (Alomone Labs, Jerusalem, Israel) were diluted and applied in HEPES-buffered extracellular solution. The drug solutions were delivered to the recorded cells by a valve-controlled fast multibarrel superfusion system with a common outlet approximately 350 μm in diameter (Automate Scientific, California, U.S.A). The application tip was routinely positioned approximately 1 mm away from and ~50 μm above the surface of the recorded cells. A computer connected to Digidata 1550B controlled the onset and duration of each drug application. The time course of the drug application was calibrated using fluorescein dye. The drugs were used at the following final concentration: BzATP and ATP (300 μM), AFC-5128 (30 nM) and JNJ-47965567 (100 nM).

Calcium Imaging

For calcium imaging, cells were loaded with Cal-520 (AAT Bioquest, California, U.S.A) by incubation with the acetoxymethyl (AM) ester form of the dye at a final concentration of 2 μM in culture media without serum. The dyes were prepared as 5 mM stock solution in DMSO and kept frozen at -20°C and diluted on the day of use. After 45 min, cells were washed several times with dye-free HEPES-buffered saline solution and transferred to an imaging chamber on a microscope (Zeiss Axio Examiner, Jena, Germany) equipped with a Zeiss 40x water immersion objective. Zen Blue imaging software (Carl Zeiss, Jena, Germany) was used for hardware control and image acquisition, and image analysis was performed using ImageJ (NIH, Maryland, U.S.A). All imaging experiments were performed at 34°C in a low divalent cation-containing bath solution with the composition (in mM): 135 NaCl, 3 KCl, 0.5 $CaCl_2$, 0.1 $MgCl_2$, 10 HEPES and 10 glucose (pH 7.2; osmolality 290–300 mmol/kg). Images were acquired at 4 Hz. Background fluorescence was measured from the cell-free area outside the soma of interest in each frame of every time series. Region of interests (ROIs) were drawn around the soma and baseline fluorescence intensity (F0) was determined by averaging 24 frames preceding the cell's exposure to BzATP or ATP and the time course of normalized fractional dye fluorescence [ΔF/F0] was obtained, where ΔF equals F(t) - F0.

Western blot

Western blot was carried out as described before [43]. Samples were prepared by homogenizing hiPSC-derived astrocytes in ice-cold extraction buffer (20 mM HEPES pH 7.4, 100 mM NaCl, 20 mM NaF, 1% Triton X-100, 1 mM sodium orthovanadate, 1 μM okadaic acid, 5 mM sodium pyrophosphate, 30 mM β-glycerophosphate, 5 mM EDTA, protease inhibitors (Complete, Roche, Cat. No 11697498001)). 15 μl of total protein were electrophoresed on 8–10% sodium dodecyl sulphate (SDS)-polyacrylamide gel, transferred to a nitrocellulose blotting membrane (Amersham Protran 0.45 μm, GE Healthcare Life Sciences) and blocked in TBS-T (150 mM NaCl, 20 mM Tris–HCl, pH 7.5, 0.1% Tween 20) supplemented with 5% non-fat dry milk. Membranes were incubated overnight at 4ºC with the rabbit anti-P2X7R primary antibody (Alomone Labs, Jerusalem, Israel, dilution 1:200) in TBS-T supplemented with 5% non-fat dry milk. On the next day, following washing with TBS-T, membranes were incubated with secondary HRP-conjugated anti-mouse or rabbit IgG (dilution 1:5000, Jackson Immuno Research, Plymouth, PA, U.S.A) and protein bands visualized using chemiluminescence (Merck Millipore, Billerica, MA, U.S.A and Pierce Biotechnology, Rockford, IL, U.S.A). Gel bands were captured using a Fujifilm LAS-4000 imaging system (Fujifilm, Tokyo, Japan). The astrocyte marker GFAP (dilution 1:500, anti-mouse; Merck, Missouri, U.S.A) was used as loading control.

Statistical analysis

The data are expressed as mean ± SEM. Statistical analysis was performed using the Mann-Whitney U test. $P < 0.05$ was considered statistically significant. All statistical analyses was performed with GraphPad Prism 9 software (GraphPad Software, San Diego, CA, U.S.A).

Results

Expression of P2X7Rs in hiPSC-derived astrocytes.

The hiPSC-derived astrocytes, which were differentiated for 4 weeks in vitro, exhibited a flat morphology (Fig. 1A). Immunocytochemical analysis at passage 7 confirmed the expression of the astrocyte marker S100β in cells maintained in astrocyte differentiation medium (Fig. 1B-D).

We also assessed the functional maturity of the hiPSC-derived astrocytes by analysis of spontaneous calcium transients. Cal-520 loaded astrocytes exhibited a weak but measurable signal for Cal-520 fluorescence indicating low resting $[Ca^{2+}]i$ (Fig. 1E). Occasionally, the hiPSC-derived astrocytes exhibited spontaneous asynchronous $[Ca^{2+}]i$ fluctuations (Fig. 1F).

To assess the expression of P2X7Rs on hiPSC-derived astrocytes, double immunostaining was performed on astrocytes at 4 weeks *in vitro* using antibodies against the astrocyte marker GFAP (Fig. 1G) and intracellular C-terminus of the P2X7R. The punctate staining pattern for P2X7R was present in GFAP-positive cells demonstrating the expression of P2X7Rs in astrocytes (Fig. 1H, I). P2X7R expression on hiPSC-derived astrocytes was further confirmed by Western blotting (Fig. 1L).

ATP evokes AFC-5128 or JNJ-47965567-sensitive Ca^{2+} transients in iPSC-derived astrocytes.

Next, we sought to assess whether P2X7Rs respond to the application of P2X7R-stimulating agonists. Previous studies have shown that the activation of the P2X7R requires high (in mM range) concentrations of ATP. The P2X7R is, however, 10 to 30 times more sensitive to the ATP analog and nonselective P2X7R agonist, 2', 3'-O-(4-benzoylbenzoyl)-ATP (BzATP) [44, 45]. We assessed the functional expression of P2X7Rs in hiPSC-derived astrocytes by monitoring changes in $[Ca^{2+}]i$ upon BzATP application, using the calcium-sensitive fluorescent reporter Cal-520. Pulse ejection of BzATP (300 μM) for 5 s evoked synchronous increase in $[Ca^{2+}]i$ (Fig. 2A).

This elevation in $[Ca^{2+}]i$ upon BzATP application persisted for a few seconds after the agonist was washed out. In support of the role for the P2X7R in mediating the intracellular $[Ca^{2+}]i$ rise, 3 min pre-incubation of astrocytes with the P2X7R antagonist AFC-5128, followed by co-application of BzATP with AFC-5128 (30 nM) significantly reduced BzATP-mediated $[Ca^{2+}]i$ response (Fig. 2A, B). We quantified the area under ΔF/F0 curve (AUC) upon BzATP application to assess the magnitude of AFC-5125-sensitive calcium transients. The results show a significant reduction in the AUC when stimulated with BzATP in the presence of AFC-5128 (Fig. 2C). Similar results were also evident when the peak amplitude of individual ΔF/F0 traces were compared (Fig. 2D, E). The endogenous P2X7R agonist ATP also induced an $[Ca^{2+}]i$ rise which was reduced by AFC-5128 (Fig. 2F, G). Both the AUC of ΔF/F0 traces and peak amplitude was also reduced upon stimulation with ATP in the presence of AFC-5128 (Fig. 2H, I).

To confirm the functional expression of P2X7Rs in hiPSC-derived astrocytes further, we repeated the BzATP application in the presence of the P2X7R antagonist JNJ-47965597 [46]. The results

demonstrated a significant reduction in the BzATP-evoked $[Ca^{2+}]i$ signals in hiPSC-derived astrocytes (Fig. 3A, B). Similar to the results observed in the presence of AFC-5128, the AUC and peak amplitude of individual ΔF/F0 traces were reduced when the astrocytes were stimulated with BzATP in the presence of JNJ-47965597 (Fig. 3C-E). ATP-evoked responses were also diminished in the presence of JNJ-47965597 (Fig. 3F, G). The AUC and peak amplitude of individual ΔF/F0 traces were significantly reduced for the period of ATP application in the presence of JNJ-47965597 (Fig. 3H, I).

In summary, our results demonstrate that Ca^{2+} entry across the plasma membrane mediated via P2X7Rs contribute to the ATP or BzATP-evoked Ca^{2+} signals and confirm the expression of functional P2X7Rs in hiPSC-derived astrocytes.

Discussion

Here, we were able to differentiate hiPSC-derived astrocytes that express functional P2X7Rs. Using fast agonist application and simultaneous Ca^{2+} imaging, we show that astrocytes respond by $[Ca^{2+}]i$ increase upon ATP and BzATP stimulation and that the selective P2X7R antagonists AFC-5128 or JNJ-47965567 abolished these effect, thereby demonstrating the expression of functional P2X7Rs in hiPSC-derived astrocytes. Therefore, the present findings support the use of hiPSC-derived astrocytes as a human brain-relevant *in vitro* model for studying ATPergic signaling, disease mechanisms and drug screening.

Despite extensive investigation into glial P2X7R expression and function in both *in vitro* and *in vivo* animal models [13, 47, 48], limited studies have been conducted to characterize expression and function of this important receptor in human astrocytes. Indeed, only two studies have reported the presence of *P2rx7* mRNA in cultured human adult and fetal brain tissue [40, 41]. The P2X7R has been proposed as a potential therapeutic target in a plethora of human conditions ranging from cancer, to cardiovascular conditions to diseases of the CNS such as neurodegenerative, psychiatric (e.g. schizophrenia, depression) and, more recently, epilepsy [49–53]. Studies investigating a causative role of P2X7R in these brain diseases have relied heavily on experimental animal models. This raises potential problems with translation since the P2X7R exhibits remarkable species-specific differences in their pharmacological properties to drugs such as AFC-5128 [42]. hiPSC-derived glia have been widely accepted as human brain-relevant *in vitro* cellular models to investigate phenotypic alterations in neurological diseases [34, 36, 54]. Thus, to advance findings from pre-clinical experimentation into the clinical setting, the development of human-derived cellular models for targeted drug screening, such as that for the P2X7R in this study, would serve an invaluable tool to bridge the gap between translational animal models and human neurological diseases.

The present study provides strong supportive evidence that hiPSC-derived astrocytes express functional P2X7Rs on their surface. This includes evidence for the expression of the receptor in the cells and imaging evidence that activation gates calcium entry which is selectively blocked by antagonists of the P2X7R. Our results therefore agree with studies showing functional P2X7R on astrocytes [55], but are in

contrast to other studies unable to detect P2X7R on astrocytes [12, 13] including work by our own group in rodents [14].

The finding that hiPSC-derived astrocytes display surface expression of P2X7Rs has important implications for signaling mechanisms in the brain in both health and disease. Both neurons and astrocytes release ATP, which is the endogenous ligand for P2X7Rs [56]. Although ATP is a low affinity ligand at P2X7Rs, [56] P2X7Rs on astrocytes may be activated by ATP released from both neighboring neurons and astrocytes leading to signal amplification. P2X7R activation on astrocytes could promote enhanced astrocyte-mediated glutamate release leading to increased network excitability. In addition, at the site of brain injury, exogenous ATP mediates the release of pro-inflammatory cytokines leading to neuroinflammation via P2X7Rs [57], possibly via upregulation of P2X7Rs during pathological conditions.

While our results suggest P2X7Rs to be functional on hiPSC-derived astrocytes, it is important to keep in mind that our studies are carried out under *in vitro* conditions and whether P2X7Rs are expressed *in vivo* in human astrocytes requires further investigation and clarification including, for example, patch clamp in human brain slices. P2X7Rs have been shown to be upregulated in human reactive astrocytes [41]. We did not detect discernable changes in morphology of astrocytes in culture over time, but did not assess if the culture conditions lead to neuroinflammation and the generation of reactive astrocytes. BzATP-evoked responses should be interpreted with caution because BzATP is a non-specific agonist at purinergic receptors and agonist activity at non-P2X7Rs has also been documented. Importantly, suggesting ATP and BzATP-mediated responses are mainly mediated via P2X7Rs, the specific P2X7R antagonists AFC-5128 or JNJ-47965567 suppressed calcium increases in astrocytes. Finally, our results should be studied in additional iPSC lines, both from healthy individuals and patients carrying potential pathogenic gene variants.

In conclusion, here we demonstrate the expression of functional P2X7Rs on hiPSCs-derived astrocytes and provide the proof-of-concept that hiPSCs represent a valid model to study P2X7Rs signaling in human cellular models.

Declarations

Ethics approval and consent to participate: The human iPSC line was obtained from Culture Collections, Public Health England, UK. Consent was obtained from the donor, by the Sanger institute that reprogrammed the fibroblasts into iPSCs and the line was distributed and used under the terms of an MTA from culture collections and RCSI.

Consent for publication: Not applicable

Availability of data and materials: The datasets used and/or analysed during the current study are available from the corresponding author on reasonable request.

Competing interests: The authors declare no conflict of interest. The funders had no role in the design of the study; in the collection, analyses, or interpretation of data; in the writing of the manuscript, or in the decision to publish the results. K.D. and M.H. are stakeholders in Lead Discovery Center GmbH and Affectis Pharmaceuticals respectively but had no influence in the study design.

Funding: This research was supported by funding from Science Foundation Ireland (17/CDA/4708 and 16/RC/3948 and co-funded under the European Regional Development Fund and by FutureNeuro industry partners), from the H2020 Marie Skłowdowksa-Curie Actions Individual Fellowship (No. 844956, 796600, 846810) and from the Irish Research Council (Government of Ireland Postdoctoral Fellowship Programme, GOIPD/2020/865 and GOIPD/2020/806).

Author Contributions: Conceptualization, J.K. and T.E.; methodology, J.K., L.D.G., M.A., A.M.M., T.E.; formal analysis, J.K.; investigation, J.K.; resources, T.E., O.W., K.D., M.H., D.H., J.H.M.P.; writing—original draft preparation, J.K., T.E.; writing—review and editing, J.K., O.W., T.E., D.H., J.H.M.P.; supervision, T.E.; project administration, T.E.; funding acquisition, J.K., T.E., D.H. and J.H.M.P. All authors have read and agreed to the published version of the manuscript.

Acknowledgements: Not applicable

References

1. Kopp, R., et al., *P2X7 Interactions and Signaling - Making Head or Tail of It*. Front Mol Neurosci, 2019. 12: p. 183.
2. Jimenez-Mateos, E.M., et al., *Regulation of P2X7 receptor expression and function in the brain*. Brain Res Bull, 2019. 151: p. 153–163.
3. Illes, P., G. Burnstock, and Y. Tang, Astroglia-Derived ATP Modulates CNS Neuronal Circuits. Trends Neurosci, 2019. 42(12): p. 885–898.
4. Cisneros-Mejorado, A., et al., *ATP signaling in brain: release, excitotoxicity and potential therapeutic targets*. Cell Mol Neurobiol, 2015. 35(1): p. 1–6.
5. Surprenant, A., *Functional properties of native and cloned P2X receptors*. Ciba Found Symp, 1996. 198: p. 208 – 19; discussion 219 – 22.
6. Solle, M., et al., *Altered cytokine production in mice lacking P2X(7) receptors*. J Biol Chem, 2001. 276(1): p. 125–32.
7. Duan, S., et al., *P2X7 receptor-mediated release of excitatory amino acids from astrocytes*. J Neurosci, 2003. 23(4): p. 1320–8.
8. Fellin, T., T. Pozzan, and G. Carmignoto, *Purinergic receptors mediate two distinct glutamate release pathways in hippocampal astrocytes*. J Biol Chem, 2006. 281(7): p. 4274–84.
9. Bardoni, R., et al., *Glutamate-mediated astrocyte-to-neuron signalling in the rat dorsal horn*. J Physiol, 2010. 588(Pt 5): p. 831–46.

10. Sperlagh, B., et al., *Involvement of P2X7 receptors in the regulation of neurotransmitter release in the rat hippocampus*. J Neurochem, 2002. 81(6): p. 1196–211.
11. Choi, S.S., et al., *Human astrocytes: secretome profiles of cytokines and chemokines*. PLoS One, 2014. 9(4): p. e92325.
12. Jabs, R., et al., *Lack of P2X receptor mediated currents in astrocytes and GluR type glial cells of the hippocampal CA1 region*. Glia, 2007. 55(16): p. 1648–55.
13. Kaczmarek-Hajek, K., et al., *Re-evaluation of neuronal P2X7 expression using novel mouse models and a P2X7-specific nanobody*. Elife, 2018. 7.
14. Morgan, J., et al., *Characterization of the Expression of the ATP-Gated P2X7 Receptor Following Status Epilepticus and during Epilepsy Using a P2X7-EGFP Reporter Mouse*. Neurosci Bull, 2020. 36(11): p. 1242–1258.
15. Sperlagh, B. and P. Illes, *P2X7 receptor: an emerging target in central nervous system diseases*. Trends Pharmacol Sci, 2014. 35(10): p. 537–47.
16. Andrejew, R., et al., *The P2X7 Receptor: Central Hub of Brain Diseases*. Front Mol Neurosci, 2020. 13: p. 124.
17. Diaz-Hernandez, M., et al., *Altered P2X7-receptor level and function in mouse models of Huntington's disease and therapeutic efficacy of antagonist administration*. FASEB J, 2009. 23(6): p. 1893–906.
18. Jimenez-Pacheco, A., et al., *Transient P2X7 Receptor Antagonism Produces Lasting Reductions in Spontaneous Seizures and Gliosis in Experimental Temporal Lobe Epilepsy*. J Neurosci, 2016. 36(22): p. 5920–32.
19. Di Lauro, C., et al., *P2X7 receptor blockade reduces tau induced toxicity, therapeutic implications in tauopathies*. Prog Neurobiol, 2022. 208: p. 102173.
20. Kovanyi, B., et al., *The role of P2X7 receptors in a rodent PCP-induced schizophrenia model*. Sci Rep, 2016. 6: p. 36680.
21. Illes, P., A. Verkhratsky, and Y. Tang, *Pathological ATPergic Signaling in Major Depression and Bipolar Disorder*. Front Mol Neurosci, 2019. 12: p. 331.
22. Donnelly-Roberts, D.L., et al., *Mammalian P2X7 receptor pharmacology: comparison of recombinant mouse, rat and human P2X7 receptors*. Br J Pharmacol, 2009. 157(7): p. 1203–14.
23. Humphreys, B.D., et al., *Isoquinolines as antagonists of the P2X7 nucleotide receptor: high selectivity for the human versus rat receptor homologues*. Mol Pharmacol, 1998. 54(1): p. 22–32.
24. Norenberg, W., et al., *Positive allosteric modulation by ivermectin of human but not murine P2X7 receptors*. Br J Pharmacol, 2012. 167(1): p. 48–66.
25. Michel, A.D., L.J. Chambers, and D.S. Walter, *Negative and positive allosteric modulators of the P2X(7) receptor*. Br J Pharmacol, 2008. 153(4): p. 737–50.
26. Hibell, A.D., et al., *Species- and agonist-dependent differences in the deactivation-kinetics of P2X7 receptors*. Naunyn Schmiedebergs Arch Pharmacol, 2001. 363(6): p. 639–48.

27. Shi, Y., et al., *Human cerebral cortex development from pluripotent stem cells to functional excitatory synapses.* Nat Neurosci, 2012. 15(3): p. 477 – 86, S1.
28. Tcw, J., et al., *An Efficient Platform for Astrocyte Differentiation from Human Induced Pluripotent Stem Cells*. Stem Cell Reports, 2017. 9(2): p. 600–614.
29. Livesey, M.R., et al., *Maturation and electrophysiological properties of human pluripotent stem cell-derived oligodendrocytes*. Stem Cells, 2016. 34(4): p. 1040–53.
30. Douvaras, P., et al., *Directed Differentiation of Human Pluripotent Stem Cells to Microglia*. Stem Cell Reports, 2017. 8(6): p. 1516–1524.
31. Schwartz, M.P., et al., *Human pluripotent stem cell-derived neural constructs for predicting neural toxicity*. Proc Natl Acad Sci U S A, 2015. 112(40): p. 12516–21.
32. Tukker, A.M., et al., *Towards animal-free neurotoxicity screening: Applicability of hiPSC-derived neuronal models for in vitro seizure liability assessment*. ALTEX, 2020. 37(1): p. 121–135.
33. Schadt, E.E., et al., *Evolving toward a human-cell based and multiscale approach to drug discovery for CNS disorders*. Front Pharmacol, 2014. 5: p. 252.
34. Rowe, R.G. and G.Q. Daley, *Induced pluripotent stem cells in disease modelling and drug discovery*. Nat Rev Genet, 2019. 20(7): p. 377–388.
35. Grskovic, M., et al., *Induced pluripotent stem cells–opportunities for disease modelling and drug discovery*. Nat Rev Drug Discov, 2011. 10(12): p. 915–29.
36. Avior, Y., I. Sagi, and N. Benvenisty, *Pluripotent stem cells in disease modelling and drug discovery*. Nat Rev Mol Cell Biol, 2016. 17(3): p. 170–82.
37. Zhao, Y.F., et al., *Astrocytes and major depression: The purinergic avenue*. Neuropharmacology, 2022. 220: p. 109252.
38. Beltran-Lobo, P., et al., *Astrocyte adaptation in Alzheimer's disease: a focus on astrocytic P2X7R.* Essays Biochem, 2022.
39. Lovelace, M.D., et al., *P2X7 receptors mediate innate phagocytosis by human neural precursor cells and neuroblasts*. Stem Cells, 2015. 33(2): p. 526–41.
40. Hashioka, S., et al., *Purinergic responses of calcium-dependent signaling pathways in cultured adult human astrocytes*. BMC Neurosci, 2014. 15: p. 18.
41. Narcisse, L., et al., *The cytokine IL-1beta transiently enhances P2X7 receptor expression and function in human astrocytes*. Glia, 2005. 49(2): p. 245–58.
42. Fischer, W., et al., *Critical Evaluation of P2X7 Receptor Antagonists in Selected Seizure Models*. PLoS One, 2016. 11(6): p. e0156468.
43. Engel, T., et al., *Bi-directional genetic modulation of GSK-3beta exacerbates hippocampal neuropathology in experimental status epilepticus*. Cell Death Dis, 2018. 9(10): p. 969.
44. North, R.A. and A. Surprenant, *Pharmacology of cloned P2X receptors*. Annu Rev Pharmacol Toxicol, 2000. 40: p. 563–80.
45. North, R.A., *Molecular physiology of P2X receptors*. Physiol Rev, 2002. 82(4): p. 1013–67.

46. Bhattacharya, A., et al., *Pharmacological characterization of a novel centrally permeable P2X7 receptor antagonist: JNJ-47965567*. Br J Pharmacol, 2013. 170(3): p. 624–40.
47. Alloisio, S., et al., *Functional evidence for presynaptic P2X7 receptors in adult rat cerebrocortical nerve terminals*. FEBS Lett, 2008. 582(28): p. 3948–53.
48. Rubini, P., et al., *Functional P2X7 receptors at cultured hippocampal astrocytes but not neurons*. Naunyn Schmiedebergs Arch Pharmacol, 2014. 387(10): p. 943–54.
49. Lucae, S., et al., *P2RX7, a gene coding for a purinergic ligand-gated ion channel, is associated with major depressive disorder*. Hum Mol Genet, 2006. 15(16): p. 2438–45.
50. Woods, L.T., et al., *Purinergic receptors as potential therapeutic targets in Alzheimer's disease*. Neuropharmacology, 2016. 104: p. 169–79.
51. Burnstock, G., *Purinergic Signalling: Therapeutic Developments*. Front Pharmacol, 2017. 8: p. 661.
52. Di Virgilio, F., *P2X7 is a cytotoxic receptor… maybe not: implications for cancer*. Purinergic Signal, 2021. 17(1): p. 55–61.
53. Beamer, E., et al., *ATP and adenosine-Two players in the control of seizures and epilepsy development*. Prog Neurobiol, 2021: p. 102105.
54. Karagiannis, P., et al., *Induced Pluripotent Stem Cells and Their Use in Human Models of Disease and Development*. Physiol Rev, 2019. 99(1): p. 79–114.
55. Zhao, Y.F., Y. Tang, and P. Illes, *Astrocytic and Oligodendrocytic P2X7 Receptors Determine Neuronal Functions in the CNS*. Front Mol Neurosci, 2021. 14: p. 641570.
56. Surprenant, A., et al., *The cytolytic P2Z receptor for extracellular ATP identified as a P2X receptor (P2X7)*. Science, 1996. 272(5262): p. 735–8.
57. Ferrari, D., et al., *The P2X7 receptor: a key player in IL-1 processing and release*. J Immunol, 2006. 176(7): p. 3877–83.

Figures

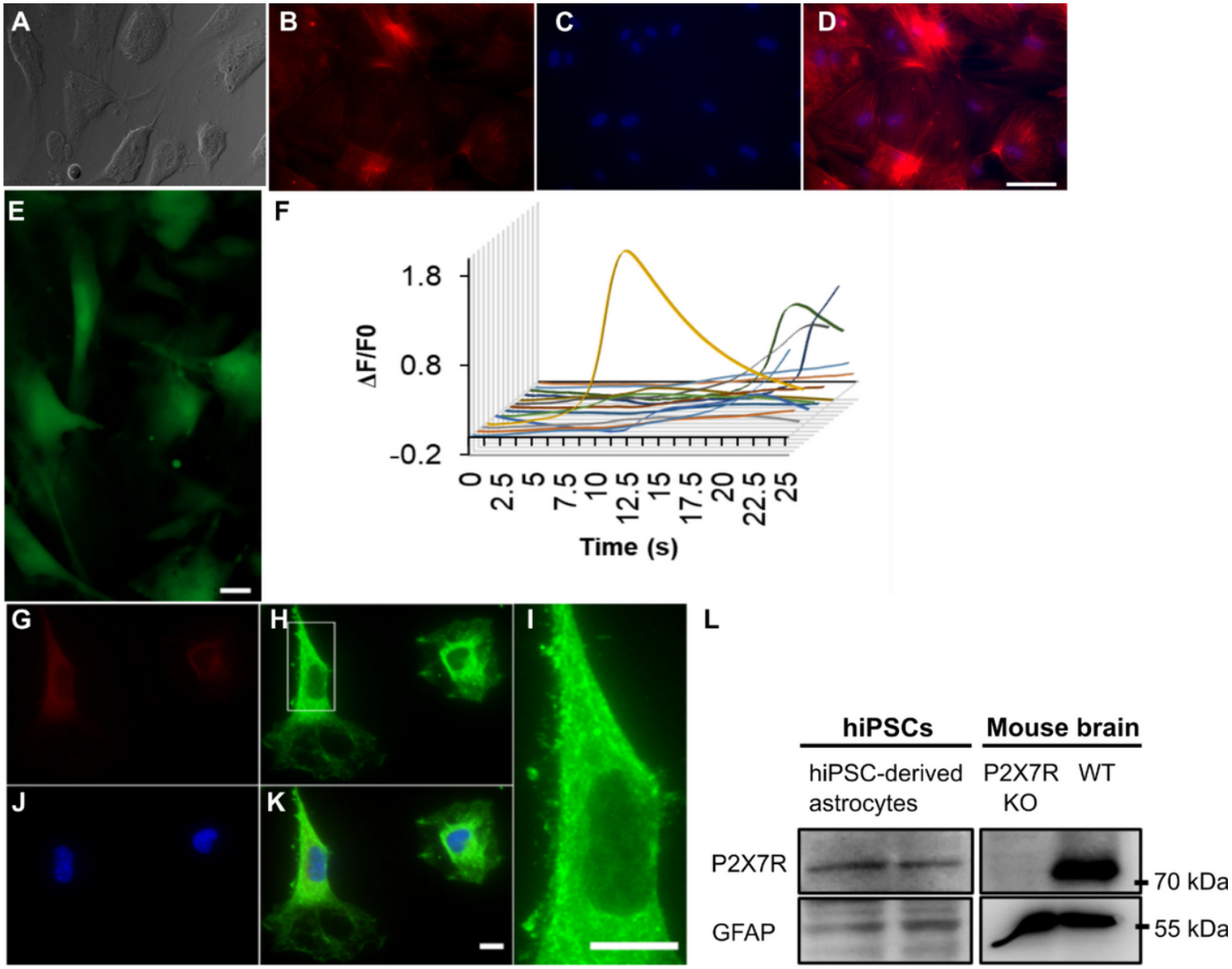

Figure 1

P2X7R expression in hiPSC-derived astrocytes. **A** Brightfield image of differentiated astrocytes. **B**Differentiated astrocytes express astrocyte marker S100β. **C** Cell nuclei stained with Hoechst (blue). **D** Merge of Hoechst (blue) and S100β (red). **E** Representative fluorescence image of astrocytes loaded with Cal-520. **F** Exemplary traces depicting spontaneous calcium transients in hiPSC-derived astrocytes. **G** Immunofluorescence analysis of hiPSC-derived astrocytes using antibodies directed against the P2X7Rs (**H,I,K**, green) with double-labelling using the astrocyte marker GFAP (G, red). Nucleus is counterstained with Hoechst (**J-K**, blue). Note the punctate co-localization of P2X7R immunoreactivity and GFAP. **L** Western blot images of P2X7R protein expressed by hiPSC-derived astrocytes and wild-type (WT) and P2X7R knock-out (KO) mouse hippocampi as positive and negative control. Scale bar 50 µm in **A-D** and **G-K** and 20 µM in **E**.

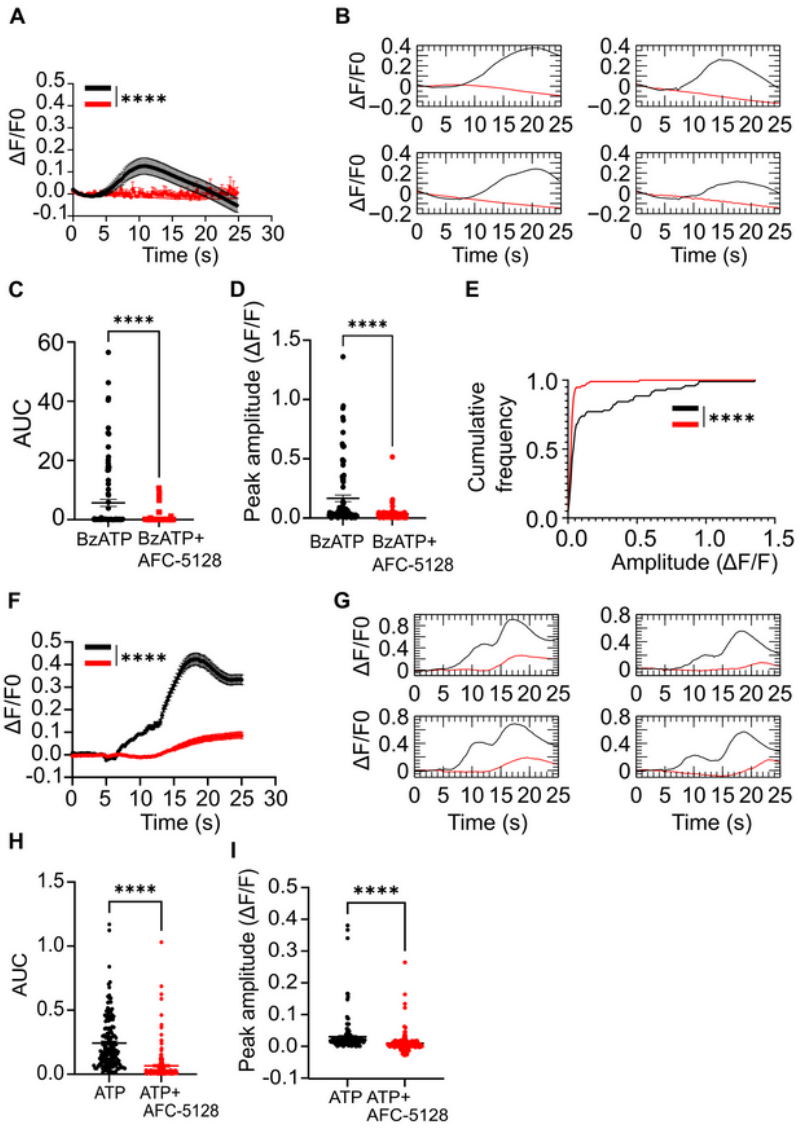

Figure 2

ATP-evoked Ca^{2+} responses in hiPSC-derived astrocytes. **A** Average time series showing response of astrocytes to the application of BzATP (300 µM) in the absence (black trace) and presence (red trace) of AFC-5128 (30 nM). (Mann-Whitney U Test, $p < 0.0001$ ($n = 96$)). **B** Exemplary ΔF/F0 traces illustrating the effect of AFC-5128 (30 nM) on BzATP-evoked calcium transients. **C** Quantitative analysis of the ATP-evoked Ca^{2+} area under the curve (AUC) during BzATP or BzATP and AFC-5128 application (Mann-

Whitney U Test, p < 0.0001 (n = 96)). **D** Quantitative analysis of the individual peak ΔF/F0 during BzATP or BzATP and AFC-5128 application (Mann-Whitney U Test, p < 0.0001 (n = 96)). **E** Cumulative frequency distribution of the amplitude of Ca^{2+} events during BzATP or BzATP and AFC-5128 application (Kolmogorov-Smirnov test, p < 0.0001 (n=96)). **F** Average time series showing response of astrocytes to the application of ATP (300 μM) in the absence (black trace) and presence (red trace) of AFC-5128 (30 nM). (Mann-Whitney U Test, p < 0.0001 (n =159)) **G** Exemplary ΔF/F0 traces illustrating the effect of AFC-5128 (30 nM) on ATP-evoked calcium transients. **H** Quantitative analysis of the ATP-evoked Ca^{2+} area under the curve during ATP or ATP and AFC-5128 application (Mann-Whitney U Test, p < 0.0001 (n =159)). **I** Quantitative analysis of the individual peak ΔF/F0 during ATP or ATP and AFC-5128 application (Mann-Whitney U Test, p < 0.0001 (n =159)). All data are expressed as mean ± SEM from individual cells. ****p < 0.0001

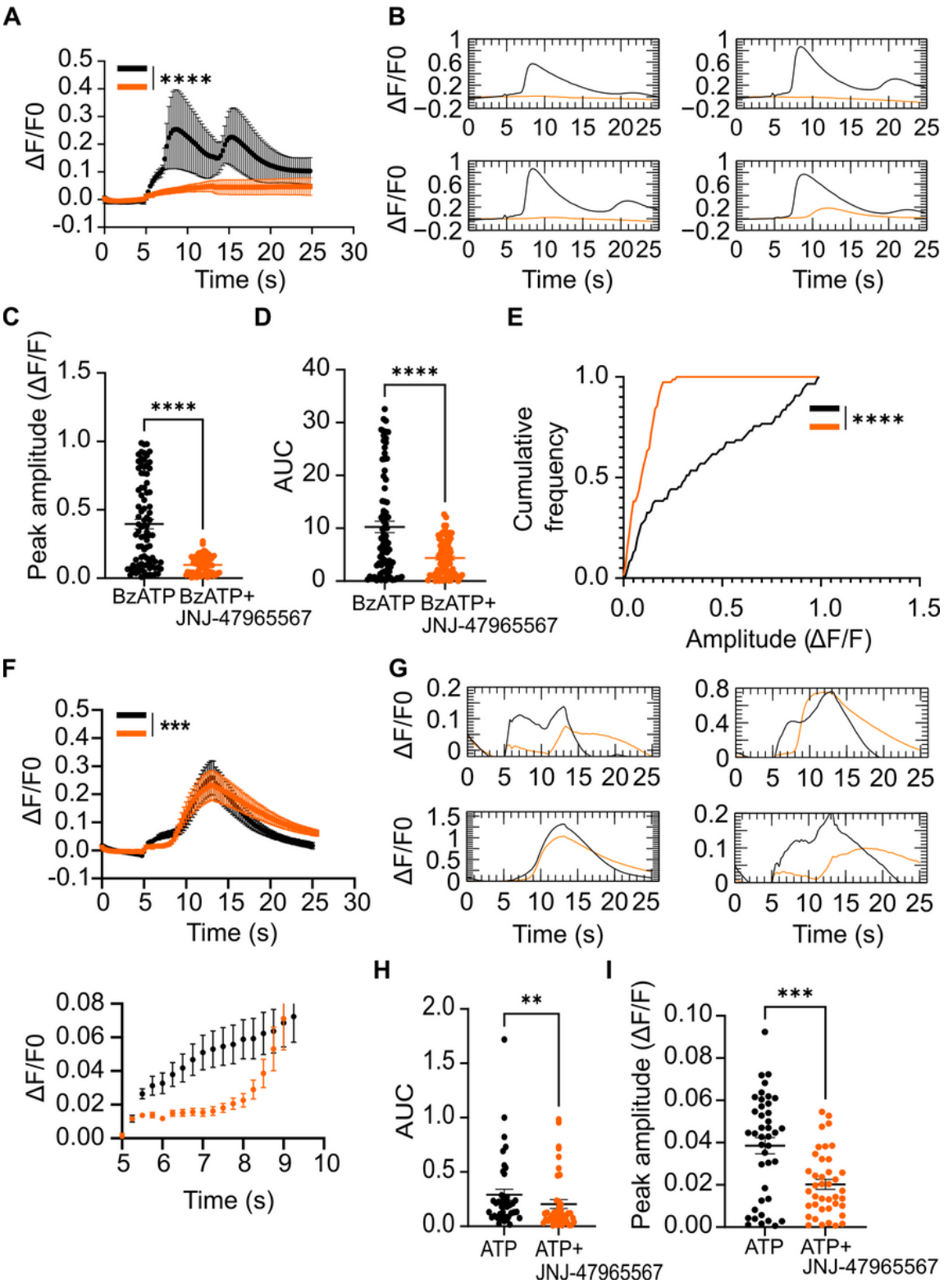

Figure 3

ATP-evoked Ca^{2+} responses in hiPSC-derived astrocytes. **A** Average time series showing response of astrocytes to the application of BzATP (300 µM) in the absence (black trace) and presence (orange trace) of JNJ-47965597 (100 nM). (Mann-Whitney U Test, p ****< 0.0001 (n = 85)). **B** Exemplary ΔF/F0 traces illustrating the effect of JNJ-47965597 (100 nM) on BzATP-evoked calcium transients. **C** Quantitative analysis of area under the curve of individual ΔF/F0 traces during BzATP or BzATP and JNJ-47965597

application (Mann-Whitney U Test, $p < 0.0009$ (n = 85)). **D** Quantitative analysis of the individual peak ΔF/F0 during BzATP or BzATP and JNJ-47965597 application (Mann-Whitney U Test, $p < 0.0001$ (n = 85). **E** Cumulative frequency distribution of the amplitude of Ca^{2+} events during BzATP or BzATP and JNJ-47965597 application (Kolmogorov-Smirnov test, $p < 0.0001$ (n = 85)). **F** Average time series showing response of astrocytes to the application of ATP (300 µM) in the absence (black trace) and presence (orange trace) of JNJ-47965597 (100 nM). The responses between 5 and 10 s are shown below. (Mann-Whitney U Test, $p < 0.0093$ (n = 85)). **G** Exemplary ΔF/F0 traces illustrating the effect of JNJ-47965597 (100 nM) on ATP-evoked calcium transients. **H** Quantitative analysis of the ATP-evoked Ca^{2+} area under the curve during ATP or ATP and JNJ-47965597 application (Mann-Whitney U Test, $p < 0.0092$ (n = 85)). **I** Quantitative analysis of the individual peak ΔF/F0 during ATP or ATP and JNJ-47965597 application (Mann-Whitney U Test, $p < 0.0007$ (n = 85)). $^{**}p < 0.01$; $^{***}p < 0.001$; $^{****}p < 0.0001$